THE JOURNAL OF PHYSICAL CHEMISTRY A

Article

pubs.acs.org/JPCA

Long-Range Chemical Sensitivity in the Sulfur K-Edge X-ray Absorption Spectra of Substituted Thiophenes

Graham N. George,*[,†] Mark J. Hackett,[†] Michael Sansone,[‡] Martin L. Gorbaty,[‡] Simon R. Kelemen,[‡] Roger C. Prince,[‡] Hugh H. Harris,[§] and Ingrid J. Pickering[†]

[†]Molecular and Environmental Sciences Group, Department of Geological Sciences, University of Saskatchewan, Saskatoon, Saskatchewan S7N 5E2, Canada

[‡]ExxonMobil Research and Engineering Company, Annandale, New Jersey 08801, United States

[§]School of Chemistry and Physics, The University of Adelaide, Adelaide, South Australia 5005, Australia

Supporting Information

ABSTRACT: Thiophenes are the simplest aromatic sulfur-containing compounds and are stable and widespread in fossil fuels. Regulation of sulfur levels in fuels and emissions has become and continues to be ever more stringent as part of governments' efforts to address negative environmental impacts of sulfur dioxide. In turn, more effective removal methods are continually being sought. In a chemical sense, thiophenes are somewhat obdurate and hence their removal from fossil fuels poses problems for the industrial chemist. Sulfur K-edge X-ray absorption spectroscopy provides key information on thiophenic components in fuels. Here we present a systematic study of the spectroscopic sensitivity to chemical modifications of the thiophene system. We conclude that while the utility of sulfur K-edge X-ray absorption spectra in understanding the chemical composition of sulfur-containing fossil fuels has already been demonstrated, care must be exercised in interpreting these spectra because the assumption of an invariant spectrum for thiophenic forms may not always be valid.

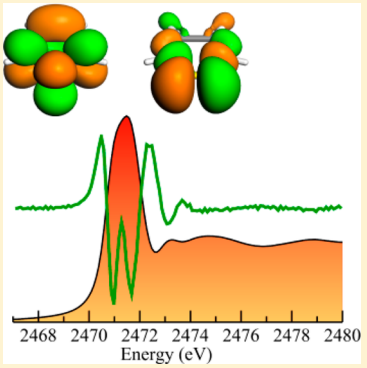

1. INTRODUCTION

Thiophenes (Figure 1) are the prototypical sulfur-containing aromatic compounds. They are electron-rich entities in which

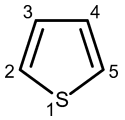

Figure 1. Schematic structure of thiophene, showing the ring numbering.

sulfur provides two electrons toward the aromatic sextet and are very stable relative to other organosulfur compounds. Sulfur-containing fossil fuels such as coals and crude oils contain considerable quantities of thiophenic compounds,[1,2] the removal of which poses challenges for the industrial chemist.[3] Worldwide, many countries have enacted legislation and regulations aimed at limiting sulfur dioxide emissions resulting from fossil fuel combustion. As a result of lower sulfur transportation fuels as well as equipment and fuel choices at power plants, sulfur dioxide emissions have decreased in North America, Europe, Japan, and Australia, with the majority of global emissions now coming from China and India.[4]

Sulfur dioxide emissions are associated with a range of adverse environmental consequences such as acid rain,[5] poor air quality, and consequential impacts on human and animal health.[6] Atmospheric sulfur dioxide is also a source of atmospheric sulfate aerosols of high albedo, which in turn can act as cloud condensation nuclei,[7] such that sulfur dioxide release from burning fossil fuels may result in increased cloud cover.[7,8] It has been suggested that increased cloud cover and consequential increases in albedo arising from sulfur emissions from burning fossil fuels may have served to mitigate temperature increases possibly caused by increased atmospheric carbon dioxide also from burning fossil fuels.[7,8] However, the adverse consequences of atmospheric sulfur emissions likely considerably outweigh any such easing.

Understanding the chemical forms of sulfur present in a fuel is a prerequisite for identifying and developing cleaner fuels that can lead to further sulfur dioxide reductions. Sulfur K-edge X-ray absorption near-edge spectroscopy was applied early to the study of fossil fuels[9,10] and is now a well-established tool for chemical speciation of complex mixtures.[11] It has been used to study the chemical forms of sulfur in a wide variety of samples, including fossil fuels, geological samples,[12] environmental systems,[13−15] archeological samples,[16] living systems such as bacteria,[17,18] plants,[19−21] fungi,[22] ascidian blood cells,[23] mammalian cell cultures,[24] and mammalian tissues.[11,25] Studies of fossil fuels include coals,[9,26] crude oils,[27,28] asphaltenes,[10] bitumens and kerogens,[29,30] source rocks,[28] and combustion

Received: June 11, 2014
Revised: August 8, 2014
Published: August 12, 2014

   dx.doi.org/10.1021/jp505766f | J. Phys. Chem. A 2014, 118, 7796−7802

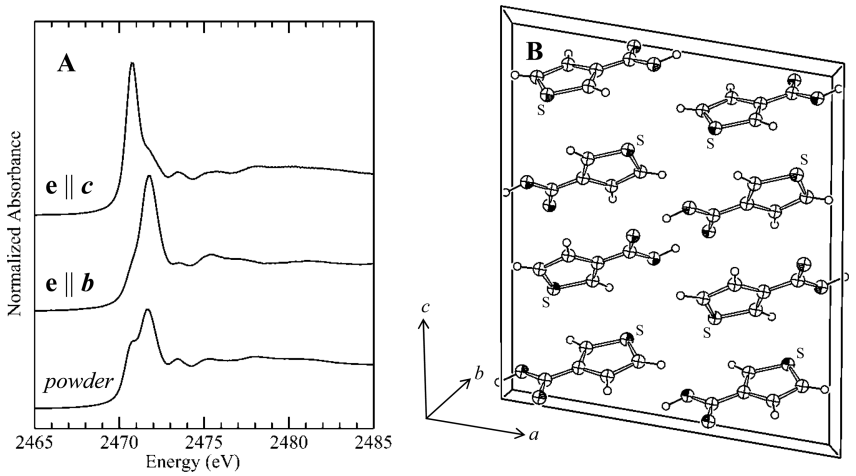

Figure 2. (A) Single crystal polarized and powder sulfur K near-edge spectra of thiophene-3-carboxylic acid, indicating substantial anisotropy of the main features in the near edge. (B) Crystal structure viewed along the crystallographic *b*-axis.

products.[31] In all of these cases the method provided essential information upon the chemical speciation of sulfur in these complex systems. Given the established importance of thiophenes in fossil fuels, and as part of an ongoing program to understand the factors leading to chemical sensitivity of sulfur K near-edge spectra, we present herein a study of the spectroscopic effects of thiophene ring substituents having different electron withdrawing and donating capacities.

2. MATERIALS AND METHODS

2.1. Samples. Thiophene, benzothiophene, dibenzothiophene, and 2- and 3-substituted thiophenes were purchased from Sigma-Aldrich Corp. and were of the highest quality available. Outer-dinaphthothiophene and inner-dinaphthothiophene were a gift from Alan Katrizky of the University of Florida. Thiophene-3-carboxylic acid was recrystallized from ethanol−water as previously described.[32,33] Appropriate single crystals were selected by microscopic examination and glued with epoxy cement to an aluminum pin that was then mounted on a goniometer. The crystal orientation matrix was determined from laboratory-based X-ray diffraction using an Enraf-Nonius CAD4 diffractometer. Solutions were prepared in toluene or isopropanol (depending on compound solubility) at concentrations of 50 mM or less and were placed in modified SPEX CertiPrep (Metuchen, NJ, USA) X-cell sample cups, employing a 6 μm thick polypropylene window. Fluorescence self-absorption artifacts in the X-ray absorption spectra[17,18] were checked for by diluting the samples by a factor of 2 and then remeasuring the spectra. Only data with no measurable self-absorption are presented in this work.

2.2. Data Collection and Analysis. Sulfur K-edge X-ray absorption spectra were recorded at the National Synchrotron Light Source (NSLS) on beamline X10C and at the Stanford Synchrotron Radiation Lightsource (SSRL) on beamlines 6−2 and 4−3. In all cases helium flight paths with 6.3 μm thick polypropylene windows were employed to minimize X-ray attenuation, and all beamlines were equipped with Si(111) double-crystal monochromators. Spectra of powdered and crystalline samples were measured at ambient temperature using total electron yield with a helium gas-amplification detector employing 500 V bias voltage, while spectra of toluene solutions were measured by monitoring the total X-ray fluorescence using a Stern-Heald-Lytle detector (The EXAFS Co., Pioche NV, USA).[34] The use of electron yield detection specifically avoids self-absorption artifacts that will be present in the fluorescence spectrum of concentrated solids[17,18] and can yield distortion-free spectra, although at poorer signal-to-noise ratio, when appropriate precautions against sample charging are taken.[18] Thus, powder samples for electron yield measurements were intimately ground with graphite, and a high bias of 500 V was used to help eliminate such artifacts.[18] The incident X-ray energy scale was calibrated by reference to the near-edge spectrum of a sodium thiosulfate standard using the literature value of 2469.2 eV as the position of the lowest energy K-edge peak.[35] The spectrum of sodium thiosulfate was also used to optimize the energy resolution, by adjusting apertures in the different beamlines. All other experimental parameters were as previously described.[18,25,26] Analysis of X-ray absorption spectroscopic data used the EXAFSPAK program suite, and calculation of unsmoothed second derivatives was done using the piecewise cubic spline method embedded within EXAFSPAK.[36]

2.3. Density Functional Theory Calculations. Density functional theory (DFT) geometry optimizations were carried out using DMol^3 Materials Studio Version 7.0[37,38] using the Perdew−Burke−Ernzerhof functional for both the potential during the self-consistent field procedure and the energy. Dmol^3 double numerical basis sets included polarization functions for all atoms with all-electron core treatments. The coordinates from these geometry optimizations were used to generate density functional theory simulations of near-edge spectra using the StoBe-deMon code[39] employing the so-called half-core-hole approximation for the core-hole, incorporating relaxation of selected excited states at the absorption edge as described by Mijovilovich et al.[40,41] Convolution with pseudo-Voigt line shape functions was conducted as previously described.[42]

3. RESULTS AND DISCUSSION

3.1. Single Crystal Polarized X-ray Absorption Near-Edge Spectra of Thiophene-3-carboxylic Acid. Previous studies of thiophene near-edge spectra[40,43,44] reported intense features at the edge corresponding to low-lying transitions that have been assigned as 1s → (S−C)π^* and 1s → (S−C)σ^*, with the former at slightly lower X-ray energy. In order to confirm these assignments we first studied single crystal polarized

dx.doi.org/10.1021/jp505766f | J. Phys. Chem. A 2014, 118, 7796−7802

spectra of thiophene-3-carboxylic acid. These are presented in Figure 2A in comparison with the spectrum of powdered crystalline thiophene-3-carboxylic acid. Two discrete peaks are observed in the powder spectrum, at 2470.6 and 2471.7 eV, which would correspond to the 1s → (S−C)π* and 1s → (S−C)σ* transitions, respectively. The previously reported crystal structure[32,33] viewed along [010] (Figure 2B) shows pairs of thiophene rings, associated by hydrogen bonding through the carboxylate groups, which are arranged in alternating planes with the ring planes inclined at 64° to each other. To a first approximation, the polarized intensity of intense dipole-allowed $\Delta l = \pm 1$ transitions is proportional to 3 $\cos^2\theta$ relative to a powder intensity of unity,[45−47] where θ is the angle between the X-ray **e**-vector and the transition dipole operator. When the **e**-vector is aligned with the crystallographic *b*- and *c*-axes, variation in the intensity of the 1s → (S−C)π* and 1s → (S−C)σ* transitions are observed showing maximal intensity along the crystallographic *c*- and *b*-axes, respectively. The 1s → (S−C)σ* should have maximal intensity when **e** is oriented along the S−C bonds which are at 56° and 5° to the *b*-axis for ($S-C_2$) and ($S-C_5$), respectively, giving rise to a transition intensity of 2.0 relative to the powder spectrum. Conversely, the 1s → (S−C)π* transition should be at maximal intensity when the **e**-vector is parallel to the normal of the planar thiophene rings. In the crystal the thiophene ring normals are closest to the crystallographic *c*-axis at ±32°, which, if the assignments are correct, should give rise to 2.2× the powder crystal intensity for the lower energy transition when **e** is oriented parallel to the crystallographic *c*-axis. The single crystal data presented here thus clearly provide direct confirmation of the previous assignments of the major transitions of the thiophene sulfur K near-edge spectra.

3.2. Effects of Ring Substituents on Thiophene Sulfur K Near-Edge Spectra. Figure 3A shows the spectra of a series of different 2- and 3-substituted thiophenes. Further spectral details are apparent when the second derivatives are examined (Figure 3B); in particular the splitting of the lowest energy major peak of the near-edge spectrum can be seen. The spectra show systematic changes with the electron withdrawing or donating capacity of the substituent, most prominently in the energies of the 1s → (S−C)π* and 1s → (S−C)σ* transitions. The positions of these transitions vary in a linear fashion with the Yukawa−Tsuno resonance component[48] of the well-known Hammett substituent constant σ,[49] often called σ_R (Figure 4),

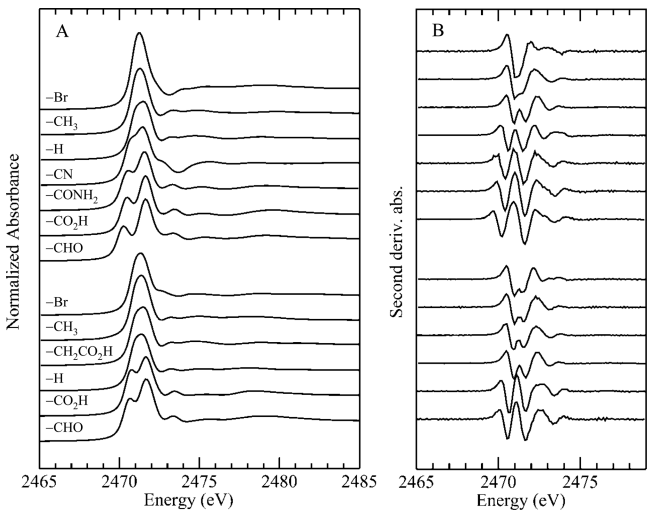

Figure 3. (A) Selected solution spectra for a variety of 2- (top) and 3-substituted (bottom) thiophenes arranged in order of increasing σ_R showing systematic changes in spectra. (B) Corresponding second derivative spectra in the same order as those shown in A.

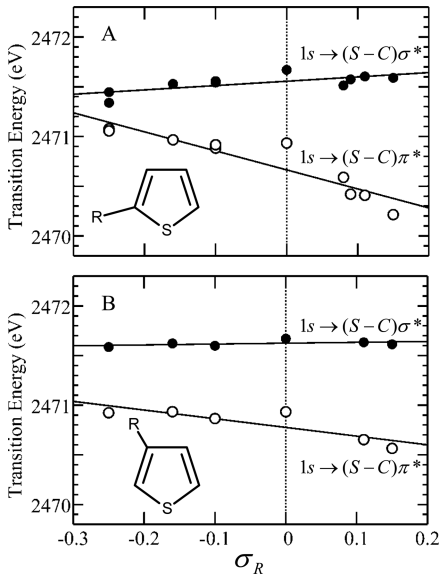

Figure 4. Relation of transition energy to σ_R. Panels A and B show the energies of 1s → (S−C)π* and 1s → (S−C)σ* transitions as a function of σ_R for 2- and 3-substituted thiophenes, respectively, determined from the second derivative minima (Figure 3). Values of σ_R are those tabulated in the literature;[49] from left to right substituents are -Br, -Cl, $-CH_3$, $-CH_2CO_2H$, $-CH_2CH_2OH$, -H, -CN, $-CONH_2$, $-CO_2H$, and -CHO for A and -Br, $-CH_3$, $-CH_2CO_2H$, -H, $-CO_2H$, and -CHO for B.

which previously has been applied to understand the kinetics of alkaline hydrolysis of thiophenic species.[50] The energies of the 1s → (S−C)π* transitions vary with σ_R substantially more than those of the 1s → (S−C)σ* transitions which are relatively insensitive to the nature of the ring substituent. As might be expected, the chemical effects are decreased with distance so that the slopes for the plots of transition energies of the 2-substituents are greater than those for the more distant 3-substituents. The energies of these transitions thus behave in a simple and systematic manner as a function of the electron withdrawing or donating capacities of the ring substituent. The graphs in Figure 4 could be used to predict the energies of these major transitions for a different substituted thiophene whose spectrum is unknown, given a known value of σ_R.

Figure 5 shows DFT simulations of the near-edge spectra of thiophene and thiophene-2-carboxylic acid, both showing reasonable correspondence with the experimental spectra. The lowest unoccupied molecular orbital (LUMO) and LUMO+1 of thiophene are B1 π* and B2 σ* orbitals, respectively. Comparison of the orbitals for thiophene and thiophene-2-carboxylic acid shows greater sensitivity of the LUMO π* to the ring substituent compared with the LUMO+1 σ* orbital which shows much more subtle changes. DFT simulations of thiophene-3-carboxylic acid give a somewhat less satisfactory match with the experimental data (Supporting Information Figure S1), indicating that the method may have difficulties when treating the effects arising from the more distant coordination. The calculated energies of the

dx.doi.org/10.1021/jp505766f | J. Phys. Chem. A 2014, 118, 7796−7802

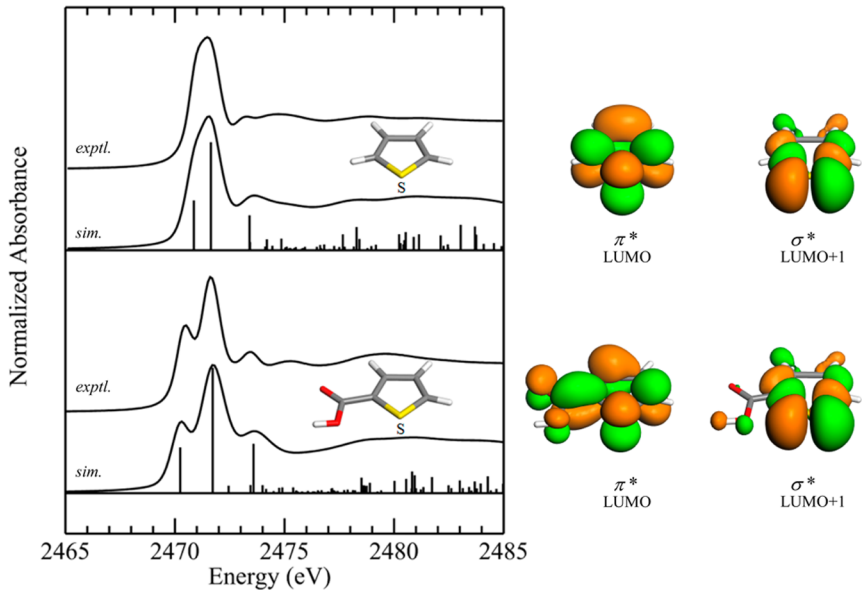

Figure 5. (Left) Comparison of experimental (exptl.) and theoretical Slater transition state simulated (sim.) spectra for thiophene and thiophene-2-carboxylic acid together with stick spectra showing the computed transitions. (Right) 0.03 electrons per cubic a.u. isosurfaces for LUMO and LUMO +1 orbitals of thiophene and thiophene-2-carboxylic acid, respectively.

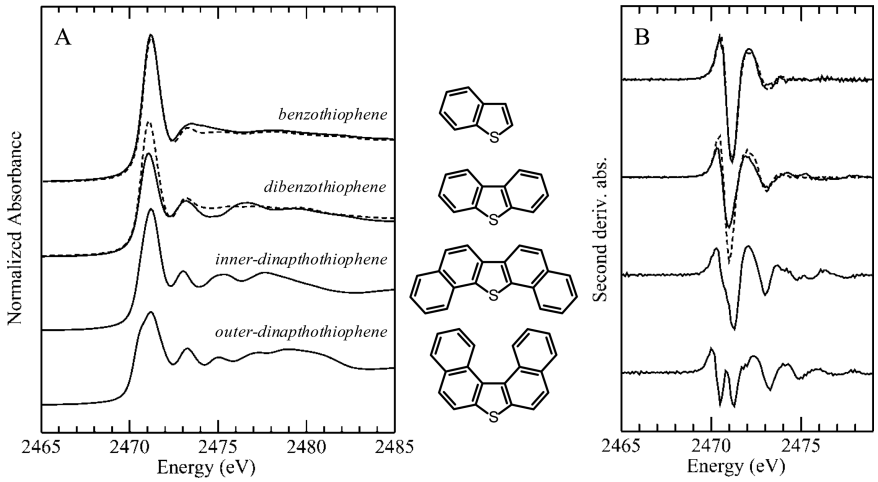

Figure 6. (A) Sulfur K near-edge X-ray absorption spectra and (B) corresponding second derivatives of four extended aromatic thiophenic compounds. Top to bottom: benzothiophene, dibenzothiophene, inner-dinaphthothiophene, and outer-dinaphthothiophene. Solid lines show electron yield spectra of powdered solids; for benzothiophene and dibenzothiophene the fluorescence spectra of toluene solutions are superimposed (broken lines).

1s → (S−C)π^* and 1s → (S−C)σ^* transitions match well with experiment for thiophene and thiophene-2-carboxylic acid, with the computed energies of the π^* transitions differing by some 0.62 eV between the two compounds, whereas those of the σ^* transitions differ by only 0.08 eV. This compares well with the respective experimental values of 0.52 and 0.07 eV. The changes in the spectra due to chemical substitution of the thiophene ring are thus due primarily to shifts in energy of the 1s → (S−C)π^* transition, while the position of the 1s → (S−C)σ^* transition remains relatively unchanged. For many thiophenes the 1s → (S−C)π^* and 1s → (S−C)σ^* transitions effectively overlap in energy, consistent with the observation of a single thiophenic peak in hydrocarbon fuels.[10,26] This may also reflect a paucity of dramatically different chemical forms in fuels compared to the chemical diversity in Figure 3.

3.3. Sulfur X-ray Absorption Near-Edge Spectra of Polycyclic Aromatic Thiophenes. In hydrocarbon fuels some fraction of the thiophenes is thought to be present in polycyclic aromatic systems; we therefore compare spectra for a series of polycyclic aromatic thiophenes in Figure 6. Figure 6 also serves to illustrate the effects of solution vs solid phase on sulfur K-edge spectra, since it compares the solid and toluene solution spectra for benzothiophene and dibenzothiophene. As has been previously observed for other chemical species,[11] the spectra of solids typically have smaller intensity for the most intense absorption peak of the near-edge spectrum, an effect which is particularly pronounced in the spectra of dibenzothiophene (Figure 6). This phenomenon has been attributed to crystal packing forces causing subtle molecular distortions relative to the solution structure, which might lift degeneracy for intense transitions.[11]

dx.doi.org/10.1021/jp505766f | J. Phys. Chem. A 2014, 118, 7796−7802

If we assume that no electron yield detection artifacts due to sample charging are present in the solid sample,[18] the differences between solid and solution are most marked for dibenzothiophene (Figure 6) and these are larger than might be expected from this explanation, because crystalline dibenzothiophene has a structure[51,52] very close to the ideal C_{2v} point group symmetry expected in solution. Thus, other phenomena such as solvent stabilization of excited states may also be important, which could be tested in future work by comparing spectra measured using solvents of different polarities. The spectra of solids also tend to have better defined structure at higher energies; this is also seen in Figure 6 and has previously been attributed to long-range-order effects.[11] Hydrocarbon fuels are in general amorphous and lack substantial long-range order. Because of these effects, solutions of standards using nonpolar solvents that mimic the fuel matrix, such as the toluene used here, are likely to be better models of the spectra of the complex amorphous system of fuels than are the analogous crystalline compounds.

The polycylic dinaphthothiophenes dinaphtho(2,1-*b*:1′,2′-*d*)thiophene and dinaphtho(1,2-*b*:2′,1′-*d*)thiophene can be conveniently and descriptively referred to by their non-IUPAC names outer- and inner-dinaphthothiophene, respectively, referring to the position of the outermost benzene ring relative to the heteroatom. The sulfur K near-edge spectra of these polycyclic aromatic systems show distinctive differences from each other and from dibenzothiophene and benzothiophene (Figure 6). In particular, outer-dinaphthothiophene shows a subtle but distinctive splitting of the primary near-edge feature with 1s → (S−C)π* and 1s → (S−C)σ* transitions at 2470.50 and 2471.25 eV, respectively. The second derivative plot of the inner-dinaphthothiophene shows that the spectrum of this compound is also split, with 1s → (S−C)π* and 1s → (S−C)σ* energies at 2470.65 and 2471.29 eV, respectively. The intensity of the σ* transition appears relatively more intense for the inner- than the outer-dinaphthothiophene.

The crystal structure of outer-dinaphthothiophene shows that the molecule is not flat but twisted in the aromatic plane due to steric overlap of the outermost benzene rings,[53] generating a structure with C_2 point group symmetry having substantial displacement of 2.7 Å of the outermost carbons in the direction normal to the thiophene ring plane. The distortion of the thiophene ring itself is quite subtle but clearly evident in the structure.[53] In contrast, the crystal structure of inner-dinaphthothiophene[54] shows the ideally planar system expected for a polycyclic aromatic species with C_{2v} point group symmetry and no stereochemically imposed distortions. Comparison of the results of ground state density functional theory calculations for both outer- and inner-dinapthothiophene indicates that, as expected, the lowered symmetry for outer-dinapthothiophene increases the spread in energies of unoccupied orbitals containing substantial 3p contributions. This is consistent with the increased spectroscopic complexity and overall broader spectrum for the outer-dinaphthothiophene. Interestingly, the intensity of the 1s → (S−C)σ* transition is substantially reduced for outer-dinaphthothiophene, compared to inner-dinaphthothiophene, and we plan to address these effects in a systematic manner for a wider range of polycyclic thiophene species in future work. Thus, we observe here that stereochemical effects can cause sufficient electronic perturbation to significantly alter the sulfur K-edge spectra of polycyclic aromatic thiophenes, although, as might be expected, the effects are more subtle than those of chemically more diverse entities shown in Figure 3.

4. CONCLUSION

Here we have investigated the factors which can cause variability in near-edge spectra of thiophenic compounds. We have used single crystal sulfur K-edge polarized spectra to confirm assignments of the major transitions and have shown that the spectra of substituted thiophenes change systematically with the nature of the substituent in a simple and quantitative manner. We also have shown that polycyclic aromatic thiophenes can have significantly different spectral characteristics. The utility of sulfur K-edge X-ray absorption spectra in understanding the chemical composition of sulfur-containing fossil fuels has already been demonstrated. The presence of a feature close to 2471.1 eV, which corresponds to the absorption maximum of dibenzothiophene, has been taken as a "fingerprint" for thiophenic forms, and efforts to quantify these have met with some success.[26] The complexity of the spectra of polycyclic species presented herein indicates that care must be exercised in interpreting spectra of hydrocarbon fuels, as the assumption of an invariant spectrum for thiophenic forms may not be valid. For liquid fuels, such as petroleum, combination with other methods[55] may be fruitful; however this may be problematic for sulfur in solid materials such as coals. We conclude that more work is required to understand the variability of sulfur spectra in fossil fuels.

■ ASSOCIATED CONTENT

Supporting Information

Figure showing the test results of the accuracy of the simulation. This material is available free of charge via the Internet at http://pubs.acs.org.

■ AUTHOR INFORMATION

Corresponding Author

*E-mail: g.george@usask.ca.

Notes

The authors declare no competing financial interest.

■ ACKNOWLEDGMENTS

Research at the University of Saskatchewan is supported by the Natural Sciences and Engineering Research Council (G.N.G. and I.J.P.), by the Canadian Institutes of Health Research (CIHR) (G.N.G. and I.J.P.), by the Saskatchewan Health Research Foundation (G.N.G. and I.J.P.), the University of Saskatchewan, and by Canada Research Chairs (G.N.G. and I.J.P.). M.J.H. is a Training in Health Research using Synchrotron Techniques (CIHR-THRUST) fellow and is supported by a CIHR Postdoctoral Fellowship and by a joint CIHR/Heart & Stroke Foundation of Canada team grant, Synchrotron Medical Imaging CIF99472. H.H.H. was supported by the Australian Research Council (Grant DP0985807-QEII). Use of the National Synchrotron Light Source, Brookhaven National Laboratory, and the Stanford Synchrotron Radiation Lightsource, SLAC National Accelerator Laboratory, are supported by the U.S. Department of Energy, Office of Science, Office of Basic Energy Sciences under Contract Nos. DE-AC02-98CH10886 and DE-AC02-76SF00515, respectively. The SSRL Structural Molecular Biology Program is supported by the DOE Office of Biological and Environmental Research and by the National Institutes of

Health, National Institute of General Medical Sciences (including Grant P41GM103393).

REFERENCES

(1) Purcell, J. M.; Juyal, P.; Kim, D.-G.; Rodgers, R. P.; Hendrickson, C. L.; Marshall, A. G. Sulfur Speciation in Petroleum: Atmospheric Pressure Photoionization or Chemical Derivatization and Electrospray Ionization Fourier Transform Ion Cyclotron Resonance Mass Spectrometry. *Energy Fuels* **2007**, *21*, 2869−2874.
(2) Liu, P.; Shi, Q.; Chung, K. H.; Zhang, Y.; Pan, N.; Zhao, S.; Xu, C. Molecular Characterization of Sulfur Compounds in Venezuela Crude Oil and Its SARA Fractions by Electrospray Ionization Fourier Transform Ion Cyclotron Resonance Mass Spectrometry. *Energy Fuels* **2010**, *24*, 5089−5096.
(3) Parkinson, G. Diesel Desulfurization Puts Refiners in a Quandary. *Chem. Eng.* **2001**, *Feb.*, 37.
(4) Kilmont, Z.; Smith, S. J.; Cofala, J. The Last Decade of Global Anthropogenic Sulfur Dioxide: 2000−2011 Emissions. *Environ. Res. Lett.* **2013**, *8*, No. 014003.
(5) Likens, G. E.; Bormann, F. H. Acid Rain: A Serious Regional Environmental Problem. *Science* **1974**, *184*, 1176−1179.
(6) Yun, Y.; Hou, L.; Sang, N. SO_2 Inhalation Modulates the Expression of Pro-inflammatory and Pro-apoptotic Genes in Rat Heart and Lung. *J. Hazard. Mater.* **2011**, *185*, 482−488.
(7) Forster, P.; Ramaswamy, V.; Artaxo, P.; Berntsen, T.; Betts, R.; Fahey, D. W.; Haywood, J.; Lean, J.; Lowe, D. C.; Myhre, G.; Nganga, J.; Prinn, R.; Raga, G.; Schulz, M.; van Dorland, R. Changes in Atmospheric Constituents and in Radiative Forcing. In *Climate Change 2007: The Physical Science Basis, Contribution of Working Group I to the Fourth Assessment Report of the Intergovernmental Panel on Climate Change*; Solomon, S., Qin, D., Manning, M., Chen, Z., Marquis, M., Avery, K. B. M., Tignor, M., Miller, H. L., Eds.; Cambridge University Press: Cambridge, U.K. and New York, NY, USA, 2007, pp 129−234.
(8) Smith, S. J.; van Aardenne, J.; Klimont, Z.; Andres, R.; Volke, A. C.; Delgado Arias, S. Anthropogenic Sulfur Dioxide Emissions. *Atmos. Chem. Phys.* **2011**, *11*, 1101−1116.
(9) Spiro, C. L.; Wong, J.; Lytle, F. W.; Greegor, R. B.; Maylotte, D. H.; Lamson, S. H. X-ray Absorption Spectroscopic Investigation of Sulfur Sites in Coal: Organic Sulfur Identification. *Science* **1984**, *226*, 48−50.
(10) George, G. N.; Gorbaty, M. L. Sulfur K Edge X-ray Absorption Spectroscopy of Petroleum Asphaltenes and Model Compounds. *J. Am. Chem. Soc.* **1989**, *111*, 3182−3186.
(11) Pickering, I. J.; Prince, R. C.; Divers, T. C.; George, G. N. Sulfur K-Edge X-ray Absorption Spectroscopy for Determining the Chemical Speciation of Sulfur in Biological Systems. *FEBS Lett.* **1998**, *441*, 11−14.
(12) Majzlan, J.; Alpers, C. N.; Koch, C. B.; McCleskey, R. B.; Myneni, S. C. B.; Neil, J. M. Vibrational, X-ray Absorption, and Moessbauer Spectra of Sulfate Minerals from the Weathered Massive Sulfide Deposit at Iron Mountain, California. *Chem. Geol.* **2011**, *284*, 296−305.
(13) Vairavamurthy, M. A.; Maletic, D.; Wang, S.; Manowitz, B.; Eglinton, T.; Lyons, T. Characterization of Sulfur-Containing Functional Groups in Sedimentary Humic Substances by X-ray Absorption Near-Edge Structure Spectroscopy. *Energy Fuels* **1997**, *11*, 546−553.
(14) Morra, M. J.; Fendorf, S. E.; Brown, P. D. Speciation of Sulfur in Humic and Fulvic Acids using X-ray Absorption Near-Edge Structure (XANES) Spectroscopy. *Geochim. Cosmochim. Acta* **1997**, *61*, 683−688.
(15) Majzlan, J.; Myneni, S. C. B. Speciation of Iron and Sulfate in Acid Waters: Aqueous Clusters to Mineral Precipitates. *Environ. Sci. Technol.* **2005**, *39*, 188−194.
(16) Fors, Y.; Jalilehvand, F.; Damian, R. E.; Bjoerdal, C.; Phillips, E.; Sandström, M. Sulfur and iron analyses of marine archaeological wood in shipwrecks from the Baltic Sea and Scandinavian waters. *J. Archaeol. Sci.* **2012**, *39*, 2521−2532.
(17) Pickering, I. J.; George, G. N.; Yu, E. Y.; Brune, D. C.; Tuschak, C.; Overmann, J.; Beatty, J. T.; Prince, R. C. Analysis of Sulfur Biochemistry of Sulfur Bacteria Using X-ray Absorption Spectroscopy. *Biochemistry* **2001**, *40*, 8138−8145.
(18) George, G. N.; Gnida, M.; Bazylinski, D. A.; Prince, R. C.; Pickering, I. J. X-ray absorption spectroscopy as a probe of microbial sulfur biochemistry: The nature of bacterial sulfur globules revisited. *J. Bacteriol.* **2008**, *190*, 6376−6383.
(19) Yu, E. Y.; Pickering, I. J.; George, G. N.; Prince, R. C. In-Situ Observation of the Generation of Isothiocyanates from Sinigrin in Horseradish and Wasabi. *Biochim. Biophys. Acta* **2001**, *1527*, 156−160.
(20) Pickering, I. J.; Wright, C.; Bubner, B.; Persans, M. W.; Yu, E. Y.; George, G. N.; Prince, R. C.; Salt, D. E. Chemical Form and Distribution of Selenium and Sulfur in the Selenium Hyperaccumulator *Astragalus bisulcatus*. *Plant Physiol.* **2003**, *131*, 1460−1467.
(21) Pickering, I. J.; Sneeden, E. Y.; Prince, R. C.; Harris, H. H.; Hirsch, G.; George, G. N. Localizing the Chemical Forms of Sulfur in Vivo Using X-ray Fluorescence Spectroscopic Imaging: Application to Onion (*Allium cepa*) Tissues. *Biochemistry* **2009**, *48*, 6846−6853.
(22) Sneeden, E. Y.; Harris, H. H.; Pickering, I. J.; Prince, R. C.; Johnson, S.; Li, X.; Block, E.; George, G. N. The Sulfur Chemistry of Shiitake Mushroom. *J. Am. Chem. Soc.* **2004**, *126*, 458−459.
(23) Frank, P.; Hedman, B.; Hodgson, K. O. XAS spectroscopy, sulfur, and the brew within blood cells from *Ascidia ceratodes*. *J. Inorg. Biochem.* **2014**, *131*, 99−108.
(24) Gnida, M.; Sneeden, E. Y.; Whitin, J. C.; Prince, R. C.; Pickering, I. J.; Korbas, M.; George, G. N. Sulfur X-ray Absorption Spectroscopy of Living Mammalian Cells: An Enabling Tool for Sulfur Metabolomics. In Situ Observation of Taurine Uptake into MDCK Cells. *Biochemistry* **2007**, *46*, 14735−14741.
(25) Hackett, M. J.; Smith, S. E.; Paterson, P. G.; Nichol, H.; Pickering, I. J.; George, G. N. X-ray Absorption Spectroscopy at the Sulfur K-Edge: A New Tool to Investigate the Biochemical Mechanisms of Neurodegeneration. *ACS Chem. Neurosci.* **2012**, *3*, 178−185.
(26) George, G. N.; Gorbaty, M. L.; Kelemen, S. R.; Sansone, M. Direct Determination and Quantification of Sulfur Forms in Coals from the Argonne Premium Sample Program. *Energy Fuels* **1991**, *5*, 93−97.
(27) Grossman, M. J.; Lee, M. K.; Prince, R. C.; Garrett, K. K.; George, G. N.; Pickering, I. J. Microbial Desulfurization of a Crude Oil Middle-Ddistillate Fraction: Analysis of the Extent of Sulfur Removal and the Effect of Removal on Remaining Sulfur. *Appl. Environ. Microbiol.* **1999**, *65*, 181−188.
(28) Waldo, G. S.; Carlson, R. M. K.; Moldowan, J. M.; Peters, K. E.; Penner-Hahn, J. E. Sulfur Speciation in Heavy Petroleums: Information from X-ray Absorption Near-Edge Structure. *Geochim. Cosmochim. Acta* **1991**, *55*, 801−814.
(29) Kelemen, S. R.; Walters, C. C.; Kwiatek, P. J.; Freund, H.; Afeworki, M.; Sansone, M.; Lamberti, W. A.; Pottorf, R. J.; Machel, H. G.; Peters, K. E. Characterization of Solid Bitumens Originating from Thermal Chemical Alteration and Thermochemical Sulfate Reduction. *Geochim. Cosmochim. Acta* **2010**, *74*, 5305−5332.
(30) Pomerantz, A. E.; Bake, K. D.; Craddock, P. R.; Kurzenhauser, K. W.; Kodalen, B. G.; Mitra-Kirtley, S.; Bolin, T. B. Sulfur Speciation in Kerogen and Bitumen from Gas and Oil Shales. *Org. Geochem.* **2014**, *68*, 5−12.
(31) Huggins, F. E.; Huffman, G. P. X-ray Absorption Fine Structure (XAFS) Spectroscopic Characterization of Emissions from Combustion of Fossil Fuels. *Int. J. Soc. Mater. Eng. Resour.* **2002**, *10*, 1−13.
(32) Hudson, P.; Robertson, J. H. The Crystal and Molecular Structure of β-Thiophenic Acid. *Acta Crystallogr.* **1964**, *17*, 1497−1505.
(33) Roux, M. V.; Temprado, M.; Jiménez, P.; Dávalos, J. Z.; Foces-Foces, C.; García, M. V.; Redondo, M. I. Thermophysical, Crystalline and Infrared Studies of the 2- and 3-Thiophenecarboxylic Acids. *Thermochim. Acta* **2003**, *404*, 235−244.

(34) Lytle, F. W.; Greegor, R. B.; Sandstron, D. R.; Marques, E. C.; Wong, J.; Spiro, C. L.; Huffman, G. P.; Huggins, F. E. Measurement of Soft X-ray Absorption Spectra with a Fluorescent Ion Chamber Detector. *Nucl. Instrum. Methods Phys. Res.* **1984**, *226*, 542−548.
(35) Sekiyama, H.; Kosugi, N.; Kuroda, H.; Ohta, T. Sulfur K-Edge Absorption Spectra of Na_2SO_4, Na_2SO_3, $Na_2S_2O_3$, and $Na_2S_2O_x$ (x=5−8). *Bull. Chem. Soc. Jpn.* **1986**, *59*, 575−579.
(36) George, G. N. 2001, http://ssrl.slac.stanford.edu/exafspak.html.
(37) Delley, B. An All-Electron Numerical Method for Solving the Local Density Functional for Polyatomic Molecules. *J. Chem. Phys.* **1990**, *92*, 508−517.
(38) Delley, B. From molecules to solids with the $DMol^3$ approach. *J. Chem. Phys.* **2000**, *113*, 7756−7764.
(39) Hermann, K.; Pettersson, L. G. M.; Casida, M. E.; Daul, C.; Goursot, A.; Koester, A.; Proynov, E.; St-Amant, A.; Salahub, D. R.; Carravetta, V.; Duarte, H.; Godbout, N.; Guan, J.; Jamorski, C.; Leboeuf, M.; Malkin, V.; Malkina, O.; Nyberg, M.; Pedocchi, L.; Sim, F.; Triguero, L.; Vela, A. *StoBe-deMon Code*, 2001.
(40) Mijovilovich, A.; Pettersson, L. G. M.; Mangold, S.; Janousch, M.; Susini, J.; Salome, M.; de Groot, F. M. F.; Weckhuysen, B. M. The Interpretation of Sulfur K-Edge XANES Spectra: A Case Study on Thiophenic and Aliphatic Sulfur Compounds. *J. Phys. Chem. A* **2009**, *113*, 2750−2756.
(41) Mijovilovich, A.; Pettersson, L. G. M.; de Groot, F. M. F.; Weckhuysen, B. M. Functional Groups and Sulfur K-Edge XANES Spectra: Divalent Sulfur and Disulfides. *J. Phys. Chem. A* **2010**, *114*, 9523−9528.
(42) Doonan, C. J.; Rubie, N. D.; Peariso, K.; Harris, H. H.; Knottenbelt, S. Z.; George, G. N.; Young, C. G.; Kirk, M. L. Electronic Structure Description of the *cis*-MoOS Unit in Models for Molybdenum Hydroxylases. *J. Am. Chem. Soc.* **2008**, *130*, 55−65.
(43) Hitchcock, A. P.; Horsley, J. A.; Stohr, J. Inner Shell Excitation of Thiophene and Thiolane: Gas, Solid, and Monolayer States. *J. Chem. Phys.* **1986**, *85*, 4835−4848.
(44) Behyan, S.; Hu, Y.; Urquhart, S. G. Sulfur 1s Near Edge X-ray Absorption Fine Structure Spectroscopy of Thiophenic and Aromatic Thioether Compounds. *J. Chem. Phys.* **2013**, *138*, 214302/1−214302/11.
(45) Heald, S. M.; Stern, E. A. Anisotropic X-ray Absorption in Layered Compounds. *Phys. Rev. B* **1977**, *16*, 5549−5559.
(46) Brouder, C. J. Angular Dependence of X-ray Absorption Spectra. *J. Phys.: Condens. Matter* **1990**, *2*, 701−738.
(47) Pickering, I. J.; George, G. N. Polarized X-ray Absorption Spectroscopy of Cupric Chloride Dihydrate. *Inorg. Chem.* **1995**, *34*, 3142−3152.
(48) Yukawa, Y.; Tsuno, Y. Resonance Effect in Hammett Relationship. II. Sigma Constants in Electrophilic Reactions and their Intercorrelation. *Bull. Chem. Soc. Jpn.* **1959**, *32*, 965−971.
(49) Taft, R. W.; Deno, N. C.; Skell, P. S. Physical Organic Chemistry. *Annu. Rev. Phys. Chem.* **1958**, *9*, 287−314.
(50) Spinelli, D.; Noto, R.; Consiglio, G.; Storace, A. Linear Free Energy Ortho-Correlations in the Thiophene Series. Part IV. Kinetics of Alkaline Hydrolysis of Some Methyl 3-Substituted Thiophene-2-carboxylates in Aqueous Methanol. *J. Chem. Soc., Perkin Trans.* **1976**, *15*, 1805−1808.
(51) Schaffrin, R. M.; Trotter, J. Structure of Dibenzothiophen. *J. Chem. Soc. A* **1970**, 1561−1565.
(52) Yamazaki, D.; Nishinaga, T.; Komatsu, K. Radical Cation of Dibenzothiophene Fully Annelated with Bicyclo[2.2.2]octene Units: X-ray Crystal Structure and Electronic Properties. *Org. Lett.* **2004**, *6*, 4179−4182.
(53) Fabbri, D.; Dore, A.; Gladiali, S.; De Lucchi, O.; Valle, G. Structure of Dinaptho[2,1-B 1′,2′-D]- 5-Membered Ring Aromatic Heterocycles. *Gazz. Chim. Ital.* **1996**, *126*, 11−18.
(54) Alam, A.; Ohta, H.; Yamamoto, T.; Ogawa, S.; Sato, R. A New Method for the Synthesis of Dinaphtho[1,2-b;2,1-d]thiophenes and Selenophenes. *Heteroat. Chem.* **2007**, *18*, 239−248.
(55) Ávila, B. M. F.; Pereira, V. B.; Gomes, A. O.; Azevedo, D. A. Speciation of Organic Sulfur Compounds using Comprehensive Two-Dimensional Gas Chromatography Coupled to Time-of-Flight Mass Spectrometry: A Powerful Tool for Petroleum Refining. *Fuel* **2014**, *126*, 188−193.